

## Electron paramagnetic resonance identification of the $\text{Sb}_{\text{Ga}}$ heteroantisite defect in GaAs:Sb

M. Baeumler, J. Schneider, and U. Kaufmann

*Fraunhofer-Institut für Angewandte Festkörperphysik Eckerstrasse 4, 7800 Freiburg, West Germany*

W. C. Mitchel

*Air Force Wright Aeronautical Laboratories, Wright-Patterson Air Force Base, Ohio 45433-6533*

P. W. Yu

*University Research Center, Wright State University, Dayton, Ohio 45435*

(Received 22 November 1988; revised manuscript received 19 January 1989)

GaAs doped with antimony (Sb) to a level of  $10^{19} \text{ cm}^{-3}$  has been studied by electron paramagnetic resonance (EPR). A new EPR spectrum has been discovered which is identified as the  $\text{Sb}_{\text{Ga}}$  heteroantisite defect. The electronic structure of this defect is practically identical with that of the intrinsic-anion antisite defects in GaP, GaAs, and InP. The EPR results show that Sb can be incorporated as an electrically active defect and therefore is not a suitable isovalent dopant in the growth of low-dislocation-density semi-insulating GaAs.

Doping of III-V compounds with non-native group-III or -V elements, so-called isovalent impurities, has attracted considerable interest as a means to reduce dislocation densities of semi-insulating materials.<sup>1</sup> In particular In doping of otherwise undoped liquid encapsulated Czochralski (LEC) GaAs has been studied extensively and has resulted in low-dislocation-density ( $< 1000 \text{ cm}^{-2}$ ) semi-insulating ( $\rho \geq 10^7 \Omega \text{ cm}$ ) GaAs:In material.<sup>2-5</sup>

To be useful in the growth of semi-insulating LEC GaAs, an isovalent dopant should be electrically inactive. However, this is not necessarily the case. Boron, for example, which is a common isovalent contaminant in LEC GaAs can be incorporated on the As site if the material is grown under Ga-rich conditions.<sup>6</sup> Thus, boron can form a heteroantisite defect  $\text{B}_{\text{As}}$  which should be electrically active as a (double) acceptor.

Antimony (Sb) doping of LEC GaAs has also been studied.<sup>1,5,7,8</sup> Such material turned out to be high-resistive *n* type but the resistivity never exceeded  $10^5 \Omega \text{ cm}$  in contrast with undoped or In-doped material. Hall effect measurements<sup>5,7,8</sup> have revealed a deep donor level at  $E_c - 0.48 \text{ eV}$  which has been attributed to the Sb dopant. It has been suggested<sup>7,8</sup> that this level might be related to the  $\text{Sb}_{\text{Ga}}$  heteroantisite.

In this Rapid Communication we will present the results of an electron-paramagnetic-resonance (EPR) study of GaAs:Sb samples grown from near stoichiometric melts. These results provide a direct confirmation of the existence of  $\text{Sb}_{\text{Ga}}$  heteroantisite defects in high concentrations and they show that this defect is electrically active. Very likely it is in fact responsible for the  $E_c - 0.48 \text{ eV}$  donor level in GaAs:Sb.

The two GaAs:Sb samples studied in this work were cut from the same ingots (*A* and *B*) as were those investigated recently by Hall effect and photoluminescence measurements.<sup>7,8</sup> Both ingots were pulled by the LEC technique from pBN crucibles. Melt *A* was slightly As rich, while melt *B* was slightly Ga rich. The ingots had room-temperature resistivities around  $10^5 \Omega \text{ cm}$  and contained a

total Sb concentration of about  $10^{19} \text{ cm}^{-3}$ . Both samples exhibited the EPR signal identified here with  $\text{Sb}_{\text{Ga}}$ . However, the signal intensity in sample *A* was a factor of 3 stronger than that in sample *B*. Therefore, all results reported here refer to sample *A*. The EPR measurements were performed at 9.5 GHz using 100-kHz field modulation and lock-in detection. Signal averaging was frequently employed to enhance the signal-to-noise ratio. The samples were mounted in a liquid-He continuous flow cryostat and could be illuminated with monochromatic light. Defect concentrations were determined from the EPR signal intensities by comparison with a sulfur doped GaP standard.

The EPR spectrum of sample *A* is shown in trace (a) of Fig. 1. Four broad lines (linewidth 39 mT) at fields of 216, 566, 708, and 767 mT are seen. They are isotropic

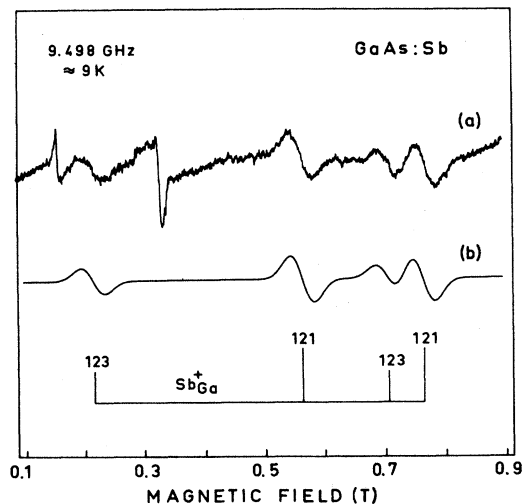


FIG. 1. (a) Measured EPR spectrum of GaAs:Sb showing four lines due to  $\text{Sb}_{\text{Ga}}^+$ . (b) Simulation of the  $\text{Sb}_{\text{Ga}}^+$  spectrum with the spin Hamiltonian parameters quoted in Table I.

and are observed in the dark. Below 9 K they start to saturate. For reasons to be given below, these four lines are identified with the  $\text{Sb}_{\text{Ga}}^+$  heteroantisite. The relatively sharp features at 157 and 326 mT are not part of the  $\text{Sb}_{\text{Ga}}^+$  spectrum, but arise from the glue used to mount the sample and from a defect near the surface, respectively. The latter signal is absent in freshly etched samples. Trace (b) in Fig. 1 is a simulation of the  $\text{Sb}_{\text{Ga}}^+$  spectrum which will be explained later.

Dramatic changes in the EPR spectrum occur when the sample is illuminated with below band-gap light. In Fig. 2 a dark spectrum is compared with a spectrum recorded after 5 s of optical excitation with  $h\nu = 1.46$  eV. After illumination the  $\text{Sb}_{\text{Ga}}^+$  lines have almost completely disappeared and a new four line spectrum has emerged which is readily recognized as that of the  $\text{As}_{\text{Ga}}^+$  antisite defect.<sup>9,10</sup> As will be discussed below these light-induced effects are fully consistent with the known optical properties of  $\text{As}_{\text{Ga}}$ .

Since Sb is isovalent with As, the defect  $\text{Sb}_{\text{As}}$  should be diamagnetic and should not give rise to an EPR spectrum. On the other hand, in full analogy with  $\text{As}_{\text{Ga}}$  in GaAs (Ref. 11) and  $\text{P}_{\text{Ga}}$  in GaP,<sup>12</sup>  $\text{Sb}_{\text{Ga}}$  is expected to be a double donor which is paramagnetic in its singly ionized charge state,  $\text{Sb}_{\text{Ga}}^+$ . The orbital part of its ground-state wave function is expected to be *s*-like and this is consistent with the observed isotropy and saturation behavior of the lines in Fig. 1(a). Therefore, a strong, isotropic Fermi contact hyperfine (hf) interaction between the electronic spin and the nuclear spins of Sb is expected. It is the observation of this hf interaction which allows an unambiguous chemical identification of the  $\text{Sb}_{\text{Ga}}$  defect.

Antimony has two isotopes  $^{121}\text{Sb}$  and  $^{123}\text{Sb}$  with natural abundancies of 57% and 43%, respectively. They have nuclear spins  $I_{121} = \frac{5}{2}$  and  $I_{123} = \frac{7}{2}$ . Thus, the spin Ham-

iltonian appropriate to analyze the spectrum in Fig. 1(a) has the form

$$\mathcal{H} = g\mu_B \mathbf{H} \cdot \mathbf{S} + A \mathbf{I} \cdot \mathbf{S} \quad (1)$$

with electronic spin  $S = \frac{1}{2}$ . The *g* factor and the hf constants  $A_{121}$ ,  $A_{123}$  are parameters to be determined from the spectrum. In zero magnetic field the hf interaction splits the  $\text{Sb}_{\text{Ga}}^+$  ground state into states of total angular momentum  $F = I \pm S = 2, 3$  for  $^{121}\text{Sb}$  and  $F = 3, 4$  for  $^{123}\text{Sb}$ . In a magnetic field these states are split and their energies are given by the eigenvalues of the above Hamiltonian for which simple analytical solutions exist.<sup>13</sup> They are plotted in the Breit-Rabi diagrams of Fig. 3. A perfect fit to the positions of the four  $\text{Sb}_{\text{Ga}}^+$  lines is obtained with the parameters *g*,  $A_{121}$ , and  $A_{123}$  as given in Table I if the lines are assigned to the four transitions shown in Fig. 3. The consistency of this assignment is easily checked by noting that the isotropic hf coupling constant *A* is given by

$$A = (8\pi/3) g g_N \mu_B \mu_N |\psi_s(0)|^2, \quad (2)$$

where  $\mu_B$  is the Bohr magneton,  $g_N$  and  $\mu_N$  are the nuclear *g* factor and nuclear magneton, respectively, and  $|\psi_s(0)|^2$  is the paramagnetic electron's density at the nucleus. Thus  $A_{121}/A_{123} = 1.84$ , as inferred from Table I, should be equal to  $g_N^{121}/g_N^{123}$ . In fact, the latter quantity, as obtained from tables of nuclear data, is 1.846. This confirms the identification of the new EPR spectrum with  $\text{Sb}_{\text{Ga}}$ . As already mentioned, the simulation in Fig. 1(b) has been performed with the  $\text{Sb}_{\text{Ga}}$  parameters listed in

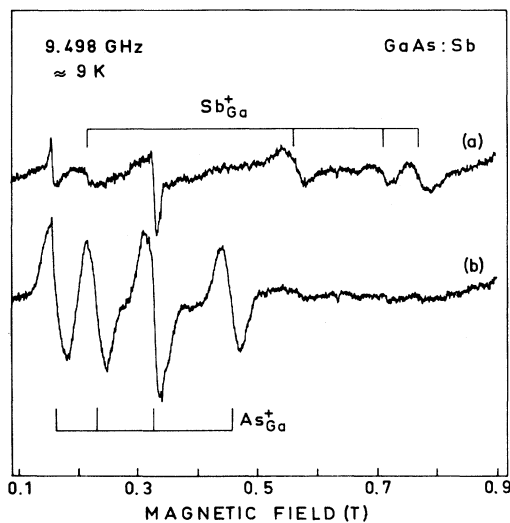


FIG. 2. EPR spectra of GaAs:Sb (a) measured in the dark and (b) measured after 5 s of illumination with  $h\nu = 1.46$  eV. The  $\text{Sb}_{\text{Ga}}^+$  concentration in (a) is very similar to that of  $\text{As}_{\text{Ga}}^+$  in (b) ( $\approx 1 \times 10^{16} \text{ cm}^{-3}$ ) although the line intensities differ significantly. This is due to the different nuclear spin multiplicities of Sb and As.

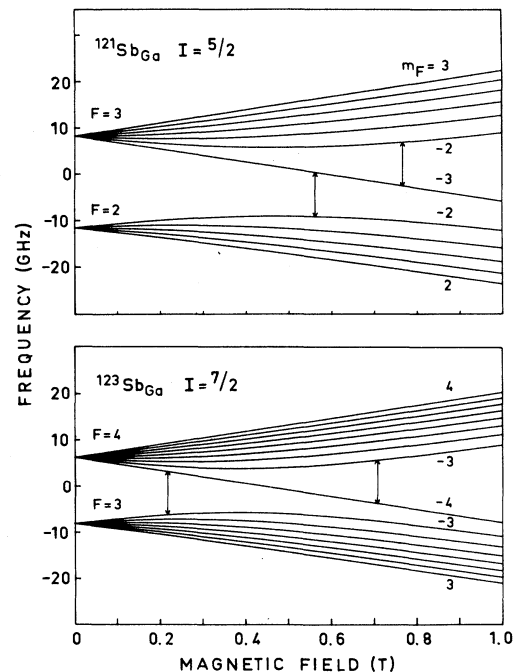


FIG. 3. Zeeman splittings of the  $\text{Sb}_{\text{Ga}}^+$  ground states (Breit-Rabi diagrams) for the isotopes  $^{121}\text{Sb}$  and  $^{123}\text{Sb}$  as obtained from the exact solutions of the Hamiltonian given in the text. Observed EPR transitions are indicated by arrows.

TABLE I: EPR parameters of antisite defects in GaP, InP, and GaAs. Note that the  $A_f$  values contain a relativistic correction which is especially prominent for Sb (Ref. 16). In this case it amounts to 52% of the unrelativistic value.

	$g$	$A$ (GHz)	$A_f$ (GHz)	$A/A_f$	Reference
GaP: $^{31}\text{P}_{\text{Ga}}$	2.007	2.90	13.31	0.218	14
InP: $^{31}\text{P}_{\text{In}}$	1.998	2.76	13.31	0.207	15
GaAs: $^{75}\text{As}_{\text{Ga}}$	2.04	2.70	14.66	0.184	9
GaAs: $^{121}\text{Sb}_{\text{Ga}}$	2.02	6.61	35.10	0.188	This work
GaAs: $^{123}\text{Sb}_{\text{Ga}}$	2.02	3.60	19.01	0.189	This work

Table I, which fix the line positions. No additional parameter is needed to fit the relative intensity of the  $^{121}\text{Sb}$  and  $^{123}\text{Sb}$  lines. This quantity is fixed by the natural abundancies and the nuclear spins of the two Sb isotopes. Although the hf splitting provides a definite chemical identification of the  $\text{Sb}_{\text{Ga}}$  defect, the EPR spectrum contains little information about the defect's surroundings. Therefore, we assume that we encounter the simplest case: namely, that of an isolated antisite  $\text{Sb}_{\text{Ga}}\text{As}_4$ . Of course, a small fraction ( $\sim 0.1\%$ ) of  $\text{Sb}_{\text{Ga}}$  may be present in the form of  $\text{Sb}_{\text{Ga}}\text{As}_3\text{Sb}$  complexes.

In Table I the spin Hamiltonian parameters of the  $\text{Sb}_{\text{Ga}}$  heteroantisite in GaAs are contrasted with those of the intrinsic anion antisites in GaP,<sup>14</sup> InP,<sup>15</sup> and GaAs.<sup>9</sup> The table also contains a column for  $A_f$  which is the value of  $A$  in Eq. (2) calculated for a single  $ns$  electron ( $n=3,4,5$  for P, As, and Sb, respectively) of the free atoms.<sup>16</sup> The ratio  $A/A_f$  represents the paramagnetic electron's density at the central atom of the antisite in question.<sup>17</sup> For all the antisites listed in Table I this density is nearly constant, varying only between 18% and 22%. In particular,  $A/A_f$  is practically identical for  $\text{As}_{\text{Ga}}^+$  and  $\text{Sb}_{\text{Ga}}^+$  in GaAs indicating that these two antisites have the same or at least nearly the same microscopic structure. This conclusion is further supported by the fact that  $\text{Sb}_{\text{Ga}}^+$  and  $\text{As}_{\text{Ga}}^+$  have practically the same EPR linewidths which are a measure for the ligand hf interaction with the four nearest-neighbor  $^{75}\text{As}$  nuclei. Thus, the wave-function localization must be very similar for  $\text{Sb}_{\text{Ga}}^+$  and  $\text{As}_{\text{Ga}}^+$ . This point seems to be important in view of the disputes about the exact microscopic nature of  $\text{As}_{\text{Ga}}$  in as-grown GaAs.<sup>10</sup>

The present data very strongly support the view that the  $E_c - 0.48$  eV donor level previously inferred from Hall measurements<sup>8</sup> on the same GaAs:Sb samples is in fact the  $\text{Sb}_{\text{Ga}}^{0,+}$  donor level. According to the Hall data this

level pins the Fermi level  $E_F$ . However, because of residual acceptors the  $\text{Sb}_{\text{Ga}}^{0,+}$  level will be partially compensated and one expects to observe the  $\text{Sb}_{\text{Ga}}^+$  EPR in the dark, but no  $\text{As}_{\text{Ga}}^+$  EPR since the  $\text{As}_{\text{Ga}}^{0,+}$  level at  $E_c - 0.75$  eV is below  $E_F$  and therefore fully occupied (neutral). This is nicely confirmed by the dark spectrum in Fig. 2(a) from which a  $\text{Sb}_{\text{Ga}}^+$  concentration of  $\approx 1 \times 10^{16} \text{ cm}^{-3}$  is obtained. From previous photo-EPR studies of  $\text{As}_{\text{Ga}}^+$  it is known that this signal in undoped semi-insulating GaAs can often be enhanced with light in the 1.4 eV range, the enhancement resulting from the process  $\text{As}_{\text{Ga}}^{0,+} + h\nu \rightarrow \text{As}_{\text{Ga}}^+ + e^-$ .<sup>11</sup> It is almost certain that the simultaneous generation of  $\text{As}_{\text{Ga}}^+$  and quenching of  $\text{Sb}_{\text{Ga}}^+$  in Fig. 2(b) is due to the above process and the subsequent trapping of the electrons at  $\text{Sb}_{\text{Ga}}^+$ . The  $\text{As}_{\text{Ga}}^+$  concentration inferred from Fig. 2(b) is  $1.2 \times 10^{16} \text{ cm}^{-3}$ . It thus appears that  $h\nu = 1.46$  eV excitation quantitatively transfers electrons from  $\text{As}_{\text{Ga}}^{0,+}$  to  $\text{Sb}_{\text{Ga}}^+$ .

The  $\text{As}_{\text{Ga}}^+$  concentration in standard undoped semi-insulating GaAs is close to  $1 \times 10^{16} \text{ cm}^{-3}$ , i.e., of the order one ppma. The  $\text{Sb}_{\text{Ga}}^+$  concentration in the samples studied here is around  $1 \times 10^{16} \text{ cm}^{-3}$ , too. Since the total Sb concentration was near  $10^{19} \text{ cm}^{-3}$ ,  $\sim 0.1\%$  of the Sb dopant atoms enter the GaAs lattice as  $\text{Sb}_{\text{Ga}}$  heteroantisites. Thus, formation of  $\text{Sb}_{\text{Ga}}$  is a factor of  $\sim 1000$  more likely than that of  $\text{As}_{\text{Ga}}$ , probably because of the more metallic character of Sb as compared to As.

In conclusion, doping of GaAs with isovalent Sb leads to the formation of  $\text{Sb}_{\text{Ga}}$  heteroantisites. At a doping level of  $10^{19} \text{ cm}^{-3}$ , about 0.1% of the dopant atoms are incorporated in this electrically active form. Comparison with previous Hall data provides very strong evidence that the  $\text{Sb}_{\text{Ga}}^{0,+}$  donor level is at  $E_c - 0.48$  eV. For this reason Sb is not a suitable isovalent dopant in the growth of semi-insulating GaAs with resistivities in the  $10^7$ - $10^8 \Omega \text{ cm}$  range.

Whether  $\text{Sb}_{\text{Ga}}$  is really a double donor, as is the case for the intrinsic antisites  $\text{As}_{\text{Ga}}$  in GaAs and  $\text{P}_{\text{Ga}}$  in GaP, remains to be investigated. In addition, it would be very desirable to know whether  $\text{Sb}_{\text{Ga}}$  exhibits metastable behavior as does  $\text{As}_{\text{Ga}}$ . If the metastability arises from an off-center motion of the antisite, as suggested for  $\text{As}_{\text{Ga}}$ ,<sup>18-20</sup> the corresponding effect for  $\text{Sb}_{\text{Ga}}$  may be impeded by size effects.

We thank J. Wagner for useful comments on the manuscript. This work has been supported by Bundesministerium für Forschung und Technologie, Bonn, West Germany, under Contract No. NT 2766 A2.

<sup>1</sup>G. Jacob, in *Semi-Insulating III-V Materials*, edited by S. Makram-Ebeid and B. Tuck (Shiva, Nantwich, England, 1982), p. 2.

<sup>2</sup>*Semi-Insulating III-V Materials*, edited by D. C. Look and J. S. Blakemore (Shiva, Nantwich, England, 1984).

<sup>3</sup>*Semi-Insulating III-V Materials*, edited by H. Kukimoto and S. Miyazawa (Ohmsha, Tokyo, 1986).

<sup>4</sup>S. McGuigan, R. N. Thomas, D. L. Barrett, G. W. Eldrige, R.

L. Messham, and B. W. Swanson, *J. Cryst. Growth* **76**, 217 (1986).

<sup>5</sup>R. N. Thomas, S. McGuigan, G. W. Eldrige, and D. L. Barrett, *Proc. IEEE* **76**, 778 (1988).

<sup>6</sup>D. W. Fischer and P. W. Yu, *J. Appl. Phys.* **59**, 1952 (1986).

<sup>7</sup>W. C. Mitchell and P. W. Yu, *J. Appl. Phys.* **57**, 623 (1985).

<sup>8</sup>W. C. Mitchell and P. W. Yu, *J. Appl. Phys.* **62**, 4781 (1987).

<sup>9</sup>R. J. Wagner, J. J. Krebs, G. H. Stauss, and A. M. White,

- Solid State Commun. **36**, 15 (1980).
- <sup>10</sup>U. Kaufmann, *GaAs and Related Compounds*, Institute of Physics Conference Series, Vol. 91 (IOP, Bristol, 1988), p. 41, and references therein.
- <sup>11</sup>B. Dischler and U. Kaufmann, *Rev. Phys. Appl.* **23**, 779 (1988), and references therein.
- <sup>12</sup>U. Kaufmann, J. Schneider, R. Wörner, T. A. Kennedy, and N. D. Wilsey, *J. Phys. C* **14**, L951 (1981).
- <sup>13</sup>G. Breit and I. I. Rabi, *Phys. Rev.* **38**, 2082 (1931).
- <sup>14</sup>U. Kaufmann, J. Schneider, and A. Räuber, *Appl. Phys. Lett.* **29**, 312 (1976).
- <sup>15</sup>T. A. Kennedy and N. D. Wilsey, *Appl. Phys. Lett.* **44**, 1089 (1984).
- <sup>16</sup>J. R. Morton and K. F. Preston, *J. Magn. Reson.* **30**, 577 (1978).
- <sup>17</sup>U. Kaufmann and J. Schneider, *Festkörperprobleme: Advances in Solid State Physics*, edited by J. Treusch, Vol. XX (Vieweg, Braunschweig, 1980), p. 87.
- <sup>18</sup>W. Kuszko, P. J. Walczak, P. Trautmann, M. Kaminska, and J. M. Baranowski, in *Defects in Semiconductors, Materials Science Forum*, edited by H. J. v. Bardeleben, Vols. 10-12 (Trans Tech, Aedermannsdorf, Switzerland, 1986), p. 317.
- <sup>19</sup>J. Dabrowski and M. Scheffler, *Phys. Rev. Lett.* **60**, 2183 (1988).
- <sup>20</sup>D. J. Chadi and K. J. Chang, *Phys. Rev. Lett.* **60**, 2187 (1988).